Hybrid Complex Projective Synchronization of Complex Chaotic Systems Using Active Control Technique with Nonlinearity in the Control Input

Milad Mohadeszadeh, Hadi Delavari*

Department of Electrical Engineering, Hamedan University of Technology, Hamedan, Iran (e-mail: m.mohadeszadeh@stu.hut.ac.ir).
**Department of Electrical Engineering, Hamedan University of Technology, Hamedan, CO 65155, Iran, (Tel: +98 81 38411523; e-mail: delavari@hut.ac.ir).*

Abstract: In this paper, the active control method based on Lyapunov function is used to study Hybrid Complex Projective Synchronization (HCPS). In the complex space, the response system is asymptotically synchronized up to the drive system by the state transformation through the use of a complex scale matrix. An extension of projective synchronization from the field of real numbers to the field of complex numbers has been done in this paper; i.e., the scaling factors are complex. The unpredictability of the scaling factors in the proposed synchronization scheme can additionally increase the security of communication. This synchronization method is studied between two non-identical complex chaotic nonlinear 3-dimensional systems. We take Lorenz system as the driving system and Chen system as the response system. In order to demonstrate the robustness of the proposed control method, dead-zone nonlinearity input is imposed to the control input. The closed loop stability conditions based on Lyapunov function and Barbalat lemma are derived. Finally, numerical simulations are presented to verify the results of the proposed scheme.

Keywords: Complex chaotic system; Hybrid complex projective synchronization; Active control; Dead-zone nonlinearity input; Lyapunov function

1. INTRODUCTION

Chaos is a very complex nonlinear phenomenon that shows some specific features such as crucially dependence to initial conditions, broad Fourier transform spectra, strange attractors and fractal properties of the motion in phase space. A tiny change in the initial conditions and the system parameters leads to an enormous difference in the long-term behavior of the system; this is the main special feature of chaotic systems (Setoudeh, 2014). Complex systems appear in many important fields of physics and engineering, for example, in the secure communication, complex variables (doubling the number of variables) can carry more transmitted information and additionally increase security of information (Mahmoud et al., 2007; Mahmoud et al., 2008). Research property of the chaotic complex system is difficult in the field of complex numbers; however, by separating the imaginary part and real part of chaotic complex system, this system can be converted to corresponding real number chaotic system. Many physical phenomena could be described by chaotic or complex chaotic systems, for example, the detuned laser systems and the amplitudes of electromagnetic fields. Several complex chaotic nonlinear systems such as complex chaotic Lorenz system (Mahmoud et al., 2007a), complex chaotic Chen and Lu systems (Mahmoud et al., 2007b) and complex chaotic coupled system (Wu et al., 2012) have been proposed in literature.

In 1990, Pecora and Carroll (Pecora and Carroll, 1990) introduced a method to synchronize two identical chaotic systems and showed that it was possible for some other chaotic systems to be completely synchronized (Faieghi and Delavari, 2012a; Faieghi et al., 2012b; Shutang and Fangfang, 2014; Sun et al., 2014). Control and synchronization of nonlinear dynamical systems like chaotic systems have attracted increasing attention in different fields, such as secure communication, optimization of nonlinear system performance, ecological systems, modeling brain activity, system identification and pattern recognition (Li et al., 2011; Florin et al., 2011; Feki, 2003; Murali and Lakshmanan, 2003; Wu and Li, 2010; Bai et al., 2005).

A wide variety of impressive approaches have been suggested in the literature for the stabilization and synchronization of the nonlinear systems such as the linear and nonlinear feedback method (Huang, 2004), time delay feedback method (Park and Kwon, 2005), back-stepping design (Wu and Lü, 2003), adaptive feedback method (Odibat, 2010), sliding mode control method (Djari, 2014; Mohadeszadeh and Delavari, 2015), fuzzy sliding mode control method (Mohadeszadeh and Delavari, 2015; Faieghi et al., 2012) and active control method (Das et al., 2013).

Various kinds of synchronization have been proposed such as complete synchronization (Zhu et al., 2009), anti-synchronization (Srivastava et al., 2014), modified generalized synchronization (Wu et al., 2012), phase synchronization (Breve et al., 2009), lag synchronization (Luo and Wang, 2013), projective synchronization (Peng et al., 2008), modified function projective synchronization (Sun et al., 2012), hybrid projective synchronization (Hu et al., 2008) and HCPS (Wei et al., 2013).

In the recent years, synchronization of dynamical systems subjected to nonlinearity control input has received a lot of attentions. In fact, the control inputs of practical systems are usually subjected to nonlinearity as a consequence of physical limitations. The presence of nonlinearity in control input was indicated to cause a serious degradation of the system performance and induce a decreasing rate of the system response (Yau and Yan, 2008a; Kebriaei and Yazdanpanah, 2010; Li et al., 2012; Márton, 2009; Yau, 2008b; Roopaei et al., 2010). In (Roopaei et al., 2010), synchronization of gyroscope system using adaptive fuzzy sliding mode control technique is investigated when dead-zone nonlinearity is imposed to the control input. In (Márton, 2009), the backlash nonlinearity is designed to impose to the control input of the motion control systems in order to analyze the control performance. But here, in this paper, we study the HCPS between two non-identical complex chaotic systems using the active control method in the presence dead-zone nonlinearity. In our contribution, we pursue four main research aims. First, finite-time convergence to the origin and stability of the proposed method are analytically proved. Second, the proposed novel scheme is achieved for complex chaotic systems; to the best of our knowledge there has been very little information about this. Third, our proposed method is designed for a wide class of complex chaotic systems, which means its universal applicability. Fourth, the robustness of the active nonlinear control method against nonlinearity in the control input is investigated for the first time.

The rest of the paper is organized as follows: Section 2 briefly describes the chaotic complex nonlinear systems. In Section 3, a general scheme of HCPS is reviewed. In Section 4, an active nonlinear controller is designed. The proposed scheme will be achieved between two non-identical complex chaotic Lorenz as drive system and Chen as response system, in Section 5. Finally, a concluding remark is given in Section 6.

2. SYSTEM DESCRIPTION

Consider the complex chaotic nonlinear Lorenz system [3] which is defined as follows:

$$\begin{cases} \dot{x}_1 = a_1(y_1 - x_1) \\ \dot{y}_1 = a_2 x_1 - y_1 - x_1 z_1 \\ \dot{z}_1 = {}^1\!/_2\,(\overline{x_1} y_1 + x_1 \overline{y_1}) - a_3 z_1 \end{cases} \tag{1}$$

where $X = (x_1, y_1, z_1)^T$ is the complex state vector, $X = X^r + jX^i$, $x_1 = {x_1}^r + j{x_1}^i$, $y_1 = {y_1}^r + j{y_1}^i$, $z_1 = {z_1}^r$, $j = \sqrt{-1}$. Dots represent derivatives with respect to time, an overbar denotes complex conjugate variables, superscripts r and i stand for the real and imaginary parts of the complex state vector X. By separating real and imaginary parts of (1), it can be represented by a 5-dimensional continuous real autonomous system as follows:

$$\begin{cases} \dot{x}_1{}^r = a_1({y_1}^r - {x_1}^r) \\ \dot{x}_1{}^i = a_1({y_1}^i - {x_1}^i) \\ \dot{y}_1{}^r = a_2 {x_1}^r - {y_1}^r - {x_1}^r {z_1}^r \\ \dot{y}_1{}^i = a_2 {x_1}^i - {y_1}^i - {x_1}^i {z_1}^r \\ \dot{z}_1{}^r = ({x_1}^r {y_1}^r + {x_1}^i {y_1}^i) - a_3 {z_1}^r \end{cases} \tag{2}$$

where a_1, a_2 and a_3 are positive parameters. System (2) exhibits a chaotic behaviour, when $(a_1, a_2, a_3)^T = (10, 28, (8/3))^T$. The chaotic attractors of (1) with initial conditions of $(2.5 + j\,6.3, 1.2 + j\,5, 0.7)^T$ are depicted in Figure 1.

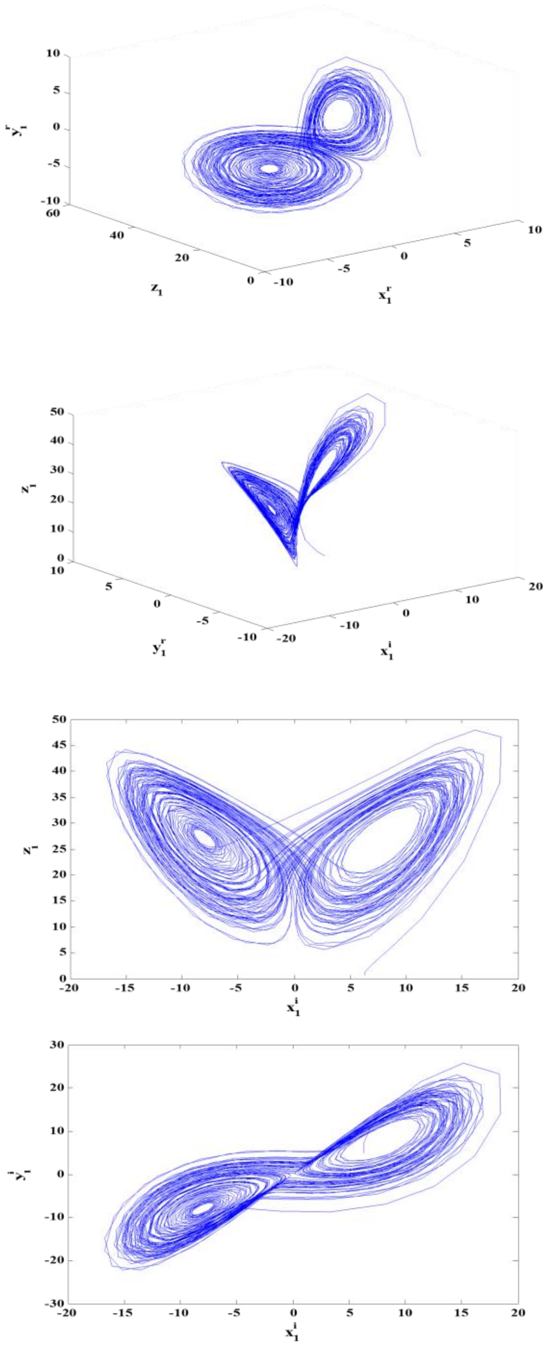

Fig. 1. 2D and 3D projections of chaotic attractors of complex chaotic Lorenz system

The complex chaotic Chen system [4] is written as:

$$\begin{cases} \dot{x}_2 = b_1(y_2 - x_2) \\ \dot{y}_2 = (b_2 - b_1)x_2 - x_2 z_2 + b_2 y_2 \\ \dot{z}_2 = {}^1\!/_2\,(\overline{x_2} y_2 + x_2 \overline{y_2}) - b_3 z_2 \end{cases} \qquad (3)$$

where $Y = (x_2, y_2, z_2)^T$ is the complex state vector, $Y = Y^r + jY^i$, $x_2 = {x_2}^r + j{x_2}^i$, $y_2 = {y_2}^r + j{y_2}^i$, $z_2 = {z_2}^r$. By separating real and imaginary parts of (3), then a 5-dimensional continuous real autonomous system can be obtained

$$\begin{cases} \dot{x}_2{}^r = b_1({y_2}^r - {x_2}^r) \\ \dot{x}_2{}^i = b_1({y_2}^i - {x_2}^i) \\ \dot{y}_2{}^r = (b_2 - b_1){x_2}^r - {x_2}^r {z_2}^r + b_2 {y_2}^r \\ \dot{y}_2{}^i = (b_2 - b_1){x_2}^i - {x_2}^i {z_2}^r + b_2 {y_2}^i \\ \dot{z}_2{}^r = ({x_2}^r {y_2}^r + {x_2}^i {y_2}^i) - b_3 {z_2}^r \end{cases} \qquad (4)$$

where b_1, b_2 and b_3 are positive parameters. When $(b_1, b_2, b_3)^T = (28, 22, 1)^T$, system (4) exhibits a chaotic behaviour. The chaotic attractors of (3) with initial conditions of $(5 + j\,1.1, 6.9 + j\,4.2, 1.5)^T$ are depicted in Figure 2.

3. A SCHEME TO ACHIEVE HCPS

Consider two non-identical complex chaotic nonlinear systems. The drive system is defined as:

$$\dot{X} = f(t, X) \qquad (5)$$

where $X \in C^n$ is a complex state vector, $f: C^n \to C^n$ is a vector of nonlinear complex functions and the response system is defined as:

$$\dot{Y} = g(t, Y) + u \qquad (6)$$

where $Y \in C^n$ is a complex state vector, $g: C^n \to C^n$ is a vector of nonlinear complex functions, $u \in C^n$ is a complex control input vector, $u = u^r + ju^i$, $u^r = ({u_1}^r, {u_2}^r, \dots, {u_n}^r)^T$, $u^i = ({u_1}^i, {u_2}^i, \dots, {u_n}^i)^T$.
In HCPS, the synchronization error between the drive system (5) and the response system (6) is defined as follows:

$$e = Y - \Lambda X \qquad (7)$$

where $e = e^r + je^i$, $e^r = ({e_1}^r, {e_2}^r, \dots, {e_n}^r)^T$, $e^i = ({e_1}^i, {e_2}^i, \dots, {e_n}^i)^T$, and $\Lambda = diag(\lambda_1, \lambda_2, \dots, \lambda_n)$ is a complex scaling matrix.

Definition 1. For the drive system (5) and the response system (6), it is said that HCPS can be achieved, if there exist a complex controller $u = u^r + ju^i$ such that:

$$lim_{t\to\infty}\|e\| = lim_{t\to\infty}\|Y - \Lambda X\| = 0 \qquad (8)$$

In (8), $\|.\|$ is the Euclidean norm of a vector. Then by separating real and imaginary parts of (8), we have

$$lim_{t\to\infty}\|e^r\| = lim_{t\to\infty}\|Y^r - \Lambda^r X^r + \Lambda^i X^i\| = 0$$

and

$$lim_{t\to\infty}\|e^i\| = lim_{t\to\infty}\|Y^i - \Lambda^r X^i - \Lambda^i X^r\| = 0$$

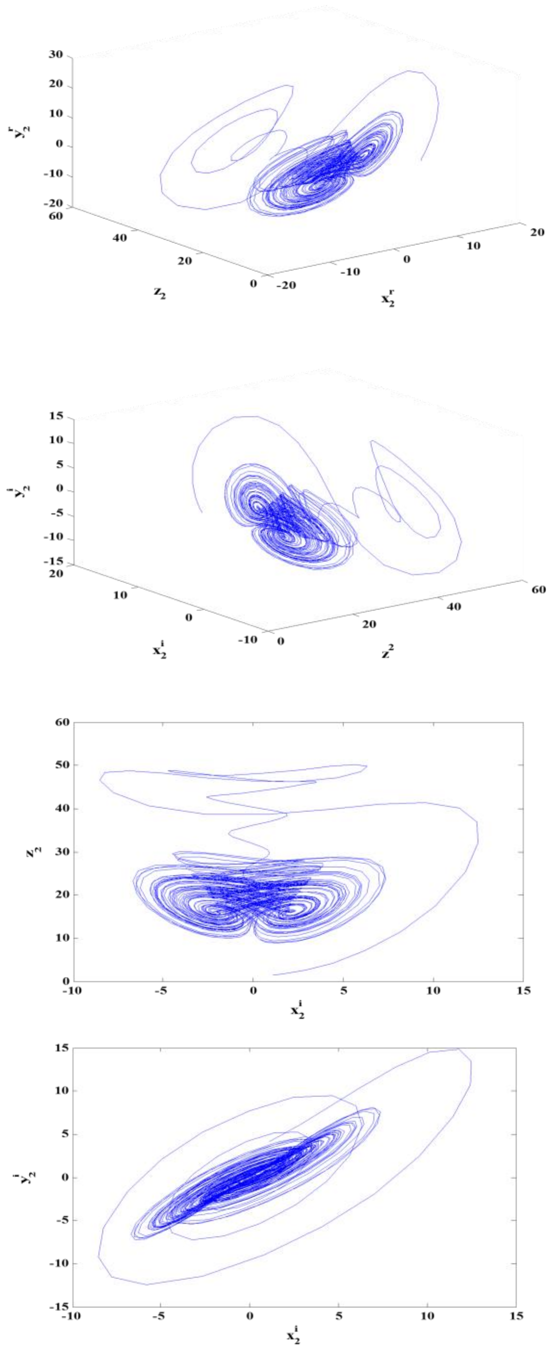

Fig. 2. 2D and 3D projections of chaotic attractors of complex chaotic Chen system

In this case, $\Lambda = \Lambda^r + j\Lambda^i = diag({\lambda_1}^r, {\lambda_2}^r, \dots, {\lambda_n}^r) + jdiag\left({\lambda_1}^i, {\lambda_2}^i, \dots, {\lambda_n}^i\right)$, ${\lambda_k}^r \in R$, ${\lambda_k}^i \in R$, $k = 1,2, \dots, n$.

3.1 HCPS of complex chaotic systems with dead-zone nonlinearity inputs

Let us consider the following two drive and response complex chaotic systems. In this case, the drive and response systems denoted by vector $X = (x_1, y_1, z_1)^T$ and $Y = (x_2, y_2, z_2)^T$, respectively. The systems are defined as:

$$\begin{cases}\dot{x}_1 = a_1(y_1 - x_1)\\ \dot{y}_1 = a_2x_1 - y_1 - x_1z_1\\ \dot{z}_1 = {}^1\!/_2\,(\overline{x_1}y_1 + x_1\overline{y_1}) - a_3z_1\end{cases} \tag{9}$$

and

$$\begin{cases}\dot{x}_2 = b_1(y_2 - x_2) + \phi_1(u_1)\\ \dot{y}_2 = (b_2 - b_1)x_2 - x_2z_2 + b_2y_2 + \phi_2(u_2)\\ \dot{z}_2 = {}^1\!/_2\,(\overline{x_2}y_2 + x_2\overline{y_2}) - b_3z_2 + \phi_3(u_3)\end{cases} \tag{10}$$

In order to investigate the robustness of the controller, dead-zone nonlinear functions $\phi_k(.)$, $k = 1,2,3$ are imposed to the control inputs u_k, $k = 1,2,3$. These nonlinear control inputs are applied to the chaotic complex system defined as:

$$\begin{cases}\phi_k(u_k{}^r) = \begin{cases}(u_k{}^r - b_+);\ u_k{}^r > b_+ ,\\ 0 \quad -b_- \le u_k{}^r \le b_+,\\ (u_k{}^r + b_-);\ u_k{}^r < -b_-\end{cases} \quad ,k = 1,2,3\\ \phi_k(u_k{}^i) = \begin{cases}(u_k{}^i - b_+);\ u_k{}^i > b_+ ,\\ 0; \quad -b_- \le u_k{}^i \le b_+,\\ (u_k{}^i + b_-);\ u_k{}^i < -b_-\end{cases} \quad ,k = 1,2\end{cases} \tag{11}$$

where b_+ and b_- are positive constants. The dead-zone nonlinearity input function depicted in Figure 3.

According to the section 3, we have the error system as follows:

$$\begin{cases}e_1 = x_2 - \lambda_1x_1\\ e_2 = y_2 - \lambda_2y_1\\ e_3 = z_2 - \lambda_3z_1\end{cases}$$

where $\lambda_1 = \lambda_1{}^r + j\lambda_1{}^i$, $\lambda_2 = \lambda_2{}^r + j\lambda_2{}^i$ and $\lambda_3 = \lambda_3{}^r$; $\lambda_k{}^r(k = 1,2,3) \in R, \lambda_k{}^i(k = 1,2) \in R$.

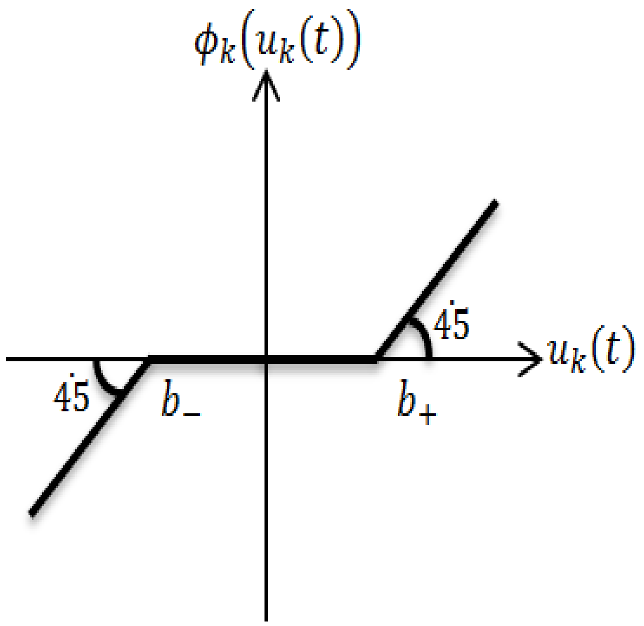

Fig. 3. A dead-zone nonlinearity input function

Therefore, the error system can be written as follows:

$$\begin{cases}e_1{}^r = x_2{}^r - \lambda_1{}^r x_1{}^r + \lambda_1{}^i x_1{}^i, \qquad (9)\\ e_1{}^i = x_2{}^i - \lambda_1{}^r x_1{}^i - \lambda_1{}^i x_1{}^r,\\ e_2{}^r = y_2{}^r - \lambda_2{}^r y_1{}^r + \lambda_2{}^i y_1{}^i,\\ e_2{}^i = y_2{}^i - \lambda_2{}^r y_1{}^i - \lambda_2{}^i y_1{}^r,\\ e_3{}^r = z_2{}^r - \lambda_3{}^r z_1{}^r\end{cases} \tag{12}$$

Using (2) and (4), the time derivative of (12) will lead to:

$$\begin{cases}\dot{\boldsymbol{e}}_{\boldsymbol{1}}{}^{\boldsymbol{r}} = b_1(e_2{}^r - e_1{}^r) + b_1\lambda_2{}^r y_1{}^r - b_1\lambda_2{}^i y_1{}^i\\ \quad -b_1\lambda_1{}^r x_1{}^r + b_1\lambda_1{}^i x_1{}^i - a_1\lambda_1{}^r y_1{}^r\\ \quad +a_1\lambda_1{}^r x_1{}^r + a_1\lambda_1{}^i y_1{}^i - a_1\lambda_1{}^i x_1{}^i + \phi_1(u_1{}^r),\\ \dot{\boldsymbol{e}}_{\boldsymbol{1}}{}^{\boldsymbol{i}} = b_1(e_2{}^i - e_1{}^i) + b_1\lambda_2{}^r y_1{}^i + b_1\lambda_2{}^i y_1{}^r\\ \quad -b_1\lambda_1{}^r x_1{}^i - b_1\lambda_1{}^i x_1{}^r - a_1\lambda_1{}^r y_1{}^i\\ \quad +a_1\lambda_1{}^r x_1{}^i - a_1\lambda_1{}^i y_1{}^r + a_1\lambda_1{}^i x_1{}^r + \phi_1(u_1{}^i),\\ \dot{\boldsymbol{e}}_{\boldsymbol{2}}{}^{\boldsymbol{r}} = (b_2 - b_1)e_1{}^r + b_2e_2{}^r + (b_2 - b_1)\lambda_1{}^r x_1{}^r\\ \quad -(b_2 - b_1)\lambda_1{}^i x_1{}^i - e_1{}^r e_3{}^r - e_1{}^r\lambda_3{}^r z_1{}^r\\ \quad -\lambda_1{}^r x_1{}^r e_3{}^r - \lambda_1{}^r x_1{}^r\lambda_3{}^r z_1{}^r + \lambda_1{}^i x_1{}^i e_3{}^r\\ \quad +\lambda_1{}^i x_1{}^i\lambda_3{}^r z_1{}^r + b_2\lambda_2{}^r y_1{}^r - b_2\lambda_2{}^i y_1{}^i\\ \quad -\lambda_2{}^r a_2x_1{}^r + \lambda_2{}^r y_1{}^r + \lambda_2{}^r x_1{}^r z_1{}^r + \lambda_2{}^i a_2x_1{}^i\\ \quad -\lambda_2{}^i y_1{}^i - \lambda_2{}^i x_1{}^i z_1{}^r + \phi_2(u_2{}^r),\\ \dot{\boldsymbol{e}}_{\boldsymbol{2}}{}^{\boldsymbol{i}} = (b_2 - b_1)e_1{}^i + b_2e_2{}^i + (b_2 - b_1)\lambda_1{}^r x_1{}^i\\ \quad +(b_2 - b_1)\lambda_1{}^i x_1{}^r - e_1{}^i e_3{}^r - e_1{}^i\lambda_3{}^r z_1{}^r\\ \quad -\lambda_1{}^r x_1{}^i e_3{}^r - \lambda_1{}^r x_1{}^i\lambda_3{}^r z_1{}^r - \lambda_1{}^i x_1{}^r e_3{}^r\\ \quad -\lambda_1{}^i x_1{}^r\lambda_3{}^r z_1{}^r + b_2\lambda_2{}^r y_1{}^i + b_2\lambda_2{}^i y_1{}^r\\ \quad -\lambda_2{}^r a_2x_1{}^i + \lambda_2{}^r y_1{}^i + \lambda_2{}^r x_1{}^i z_1{}^r - \lambda_2{}^i a_2x_1{}^r\\ \quad +\lambda_2{}^i y_1{}^r + \lambda_2{}^i x_1{}^r z_1{}^r + \phi_2(u_2{}^i),\\ \dot{\boldsymbol{e}}_{\boldsymbol{3}}{}^{\boldsymbol{r}} = -b_3e_3{}^r + e_1{}^r e_2{}^r + e_1{}^r\lambda_2{}^r y_1{}^r\\ \quad -e_1{}^r\lambda_2{}^i y_1{}^i + \lambda_1{}^r x_1{}^r e_2{}^r + \lambda_1{}^r x_1{}^r\lambda_2{}^r y_1{}^r\\ \quad -\lambda_1{}^r x_1{}^r\lambda_2{}^i y_1{}^i - \lambda_1{}^i x_1{}^i e_2{}^r - \lambda_1{}^i x_1{}^i\lambda_2{}^r y_1{}^r\\ \quad +\lambda_1{}^i x_1{}^i\lambda_2{}^i y_1{}^i + e_1{}^i e_2{}^i + e_1{}^i\lambda_2{}^r y_1{}^i\\ \quad +e_1{}^i\lambda_2{}^i y_1{}^r + \lambda_1{}^r x_1{}^i e_2{}^i + \lambda_1{}^r x_1{}^i\lambda_2{}^r y_1{}^i\\ \quad +\lambda_1{}^r x_1{}^i\lambda_2{}^i y_1{}^r + \lambda_1{}^i x_1{}^r e_2{}^i + \lambda_1{}^i x_1{}^r\lambda_2{}^r y_1{}^i\\ \quad +\lambda_1{}^i x_1{}^r\lambda_2{}^i y_1{}^r - b_3\lambda_3{}^r z_1{}^r - \lambda_3{}^r x_1{}^r y_1{}^r\\ \quad -\lambda_3{}^r x_1{}^i y_1{}^i + a_3\lambda_3{}^r z_1{}^r + \phi_3(u_3{}^r)\end{cases} \tag{13}$$

The goal of this paper is that for any given chaotic complex system, such as (9) and (10), an active nonlinear controller is designed in spite of the dead-zone nonlinear inputs $\phi_k(u_k)$, $k = 1,2,3$, such that the asymptotic stability of the resulting error dynamics system (13) can be achieved in the sense of (8)

4. ACTIVE NONLINEAR CONTROLLER DESIGN

The design procedure has two main steps. The first part is to eliminate the nonlinearity in (13) and the second step is to make the error system asymptotically stable. In fact, one of the shortcomings of active control is that an accurate knowledge of mathematical model of the system is needed, but in practical application there are always unknown factors which affect the control systems.

Theorem 1. Consider (13) without effect of dead-zone nonlinearity. Therefore, the control inputs are designed as follows:

$$\begin{cases} \boldsymbol{u_1}^r = -k_1e_1{}^r - b_1e_2{}^r - b_1\lambda_2{}^r y_1{}^r + b_1\lambda_2{}^i y_1{}^i + b_1\lambda_1{}^r x_1{}^r \\ -b_1\lambda_1{}^i x_1{}^i + a_1\lambda_1{}^r y_1{}^r - a_1\lambda_1{}^r x_1{}^r - a_1\lambda_1{}^i y_1{}^i + a_1\lambda_1{}^i x_1{}^i, \\ \boldsymbol{u_1}^i = -k_2e_1{}^i - b_1e_2{}^i - b_1\lambda_2{}^r y_1{}^i - b_1\lambda_2{}^i y_1{}^r + b_1\lambda_1{}^r x_1{}^i \\ +b_1\lambda_1{}^i x_1{}^r + a_1\lambda_1{}^r y_1{}^i - a_1\lambda_1{}^r x_1{}^i + a_1\lambda_1{}^i y_1{}^r - a_1\lambda_1{}^i x_1{}^r, \\ \boldsymbol{u_2}^r = -(b_2-b_1)e_1{}^r - (b_2+k_3)e_2{}^r - (b_2-b_1)\lambda_1{}^r x_1{}^r \\ +(b_2-b_1)\lambda_1{}^i x_1{}^i + e_1{}^r e_3{}^r + e_1{}^r\lambda_3{}^r z_1{}^r + \lambda_1{}^r x_1{}^r e_3{}^r \\ +\lambda_1{}^r x_1{}^r\lambda_3{}^r z_1{}^r - \lambda_1{}^i x_1{}^i e_3{}^r - \lambda_1{}^i x_1{}^i\lambda_3{}^r z_1{}^r - b_2\lambda_2{}^r y_1{}^r \\ +b_2\lambda_2{}^i y_1{}^i + \lambda_2{}^r a_2 x_1{}^r - \lambda_2{}^r y_1{}^r - \lambda_2{}^r x_1{}^r z_1{}^r \\ -\lambda_2{}^i a_2 x_1{}^i + \lambda_2{}^i y_1{}^i + \lambda_2{}^i x_1{}^i z_1{}^r, \\ \boldsymbol{u_2}^i = -(b_2-b_1)e_1{}^i - (b_2+k_4)e_2{}^i - (b_2-b_1)\lambda_1{}^r x_1{}^i \\ -(b_2-b_1)\lambda_1{}^i x_1{}^r + e_1{}^i e_3{}^r + e_1{}^i\lambda_3{}^r z_1{}^r + \lambda_1{}^r x_1{}^i e_3{}^r \\ +\lambda_1{}^r x_1{}^i\lambda_3{}^r z_1{}^r + \lambda_1{}^i x_1{}^r e_3{}^r + \lambda_1{}^i x_1{}^r\lambda_3{}^r z_1{}^r - b_2\lambda_2{}^r y_1{}^i \\ -b_2\lambda_2{}^i y_1{}^r + \lambda_2{}^r a_2 x_1{}^i - \lambda_2{}^r y_1{}^i - \lambda_2{}^r x_1{}^i z_1{}^r \\ +\lambda_2{}^i a_2 x_1{}^r - \lambda_2{}^i y_1{}^r - \lambda_2{}^i x_1{}^r z_1{}^r, \\ \boldsymbol{u_3}^r = -k_5e_3{}^r - e_1{}^r e_2{}^r - e_1{}^r\lambda_2{}^r y_1{}^r + e_1{}^r\lambda_2{}^i y_1{}^i \\ -\lambda_1{}^r x_1{}^r e_2{}^r - \lambda_1{}^r x_1{}^r\lambda_2{}^r y_1{}^r + \lambda_1{}^r x_1{}^r\lambda_2{}^i y_1{}^i + \lambda_1{}^i x_1{}^i e_2{}^r \\ +\lambda_1{}^i x_1{}^i\lambda_2{}^r y_1{}^r - \lambda_1{}^i x_1{}^i\lambda_2{}^i y_1{}^i - e_1{}^i e_2{}^i - e_1{}^i\lambda_2{}^r y_1{}^i \\ -e_1{}^i\lambda_2{}^i y_1{}^r - \lambda_1{}^r x_1{}^i e_2{}^i - \lambda_1{}^r x_1{}^i\lambda_2{}^r y_1{}^i - \lambda_1{}^r x_1{}^i\lambda_2{}^i y_1{}^r \\ -\lambda_1{}^i x_1{}^r e_2{}^i - \lambda_1{}^i x_1{}^r\lambda_2{}^r y_1{}^i - \lambda_1{}^i x_1{}^r\lambda_2{}^i y_1{}^r \\ +b_3\lambda_3{}^r z_1{}^r + \lambda_3{}^r x_1{}^r y_1{}^r + \lambda_3{}^r x_1{}^i y_1{}^i - a_3\lambda_3{}^r z_1{}^r \end{cases} \tag{14}$$

where $k_i > 0, i = 1,2,\dots,5$. Then, HCPS is achieved between the drive and the slave systems, (9) and (10) respectively; i.e., the error state vector (13) converge to zero.

Proof. The stability of (13) can be proven as follows:
Substituting nonlinear controllers (14) into (13) yields the linear error dynamics as:

$$\begin{cases} \dot{\boldsymbol{e}}_{\boldsymbol{1}}{}^r = -(b_1+k_1)e_1{}^r, \\ \dot{\boldsymbol{e}}_{\boldsymbol{1}}{}^i = -(b_1+k_2)e_1{}^i, \\ \dot{\boldsymbol{e}}_{\boldsymbol{2}}{}^r = -(k_3)e_2{}^r, \\ \dot{\boldsymbol{e}}_{\boldsymbol{2}}{}^i = -(k_4)e_2{}^i, \\ \dot{\boldsymbol{e}}_{\boldsymbol{3}}{}^r = -(b_3+k_5)e_3{}^r \end{cases} \tag{15}$$

1: By constructing the positive Lyapunov function candidate as

$$V(t) = {}^1\!/_2\left(\sum_{k=1}^{3}(e_k{}^r)^2 + \sum_{k=1}^{2}(e_k{}^i)^2\right) \tag{16}$$

Taking time derivative of (16), results

$$\dot V(t) = e_1{}^r\dot e_1{}^r + e_1{}^i\dot e_1{}^i + e_2{}^r\dot e_2{}^r + e_2{}^i\dot e_2{}^i + e_3{}^r\dot e_3{}^r \tag{17}$$

By inserting (15) into (17), we have

$$\dot V(t) = -(b_1+k_1)(e_1{}^r)^2 - (b_1+k_2)(e_1{}^i)^2 - k_3(e_2{}^r)^2 - k_4(e_2{}^i)^2 - (b_3+k_5)(e_3{}^r)^2 \tag{18}$$

Therefore, if $k_1 > -b_1$, $k_2 > -b_1$, $k_3 > 0$, $k_4 > 0$ and $k_5 > -b_3$, then the right side of (18) is negative. Thus the closed loop system is asymptotically stable.
2: The error dynamic (15) can be written as follows:

$$\dot E = AE$$

where $E = (e_1{}^r, e_1{}^i, e_2{}^r, e_2{}^i, e_3{}^r)^T$, $A = diag(-(b_1+k_1), -(b_1+k_2), -k_3, -k_4, -(b_3+k_5))$
Now, we can choose the control parameters $k_i, i = 1,2,\dots,5$ such that all eigenvalues $\lambda_i, i = 1,2,\dots,5$ of A satisfy the condition:

$$|arg(\lambda_i)| > {}^{\pi}\!/_2$$

i.e., the time derivative of (16) is negative definite. Therefore, zero solution of the error dynamics system (15) is asymptotically stable.
3: According to Barabalat's lemma, if $e_k{}^r, k = 1,2,3$ and $e_k{}^i, k = 1,2$ have finite values as $t \to \infty$ and if $(\dot e_k{}^r, \dot e_k{}^i)$ are uniformly continuous, then $\dot e_k{}^r$ and $\dot e_k{}^i$ tend to zero as $t \to \infty$. The consequence of this lemma is that if $(e_k{}^r, e_k{}^i) \in L_2[0,\infty)$ and $(\dot e_k{}^r, \dot e_k{}^i)$ are bounded, then $e_k{}^r$ and $e_k{}^i$ tend to zero as $t \to \infty$. Since this is indeed true, $e_k{}^r$ and $e_k{}^i$ tend to zero as $t \to \infty$.
Hence the proof is achieved.
The next step is to design an active nonlinear controller, when the control input function contains dead-zone nonlinearity. Assume that $u_k = u_k{}^r + ju_k{}^i$, $k = 1,2,3$ are as follow:

$$\begin{cases} u_k{}^r = \begin{cases} -\beta\mu_k{}^r sgn(e_k{}^r) - b_-; & e_k{}^r > 0 \\ 0; & e_k{}^r = 0 \\ -\beta\mu_k{}^r sgn(e_k{}^r) + b_+; & e_k{}^r < 0 \end{cases}, \quad k = 1,2,3 \\ u_k{}^i = \begin{cases} -\beta\mu_k{}^i sgn(e_k{}^i) - b_-; & e_k{}^i > 0 \\ 0; & e_k{}^i = 0 \\ -\beta\mu_k{}^i sgn(e_k{}^i) + b_+; & e_k{}^i < 0 \end{cases}, \quad k = 1,2 \end{cases} \tag{19}$$

By assuming, $\mu_k = \mu_k{}^r + j\mu_k{}^i$, $k = 1,2,3$ are as follow:

$$\begin{cases} \mu_1{}^r = \begin{pmatrix} |b_1(e_2{}^r - e_1{}^r) + b_1\lambda_2{}^r y_1{}^r - b_1\lambda_2{}^i y_1{}^i \\ -b_1\lambda_1{}^r x_1{}^r + b_1\lambda_1{}^i x_1{}^i - a_1\lambda_1{}^r y_1{}^r \\ +a_1\lambda_1{}^r x_1{}^r + a_1\lambda_1{}^i y_1{}^i - a_1\lambda_1{}^i x_1{}^i| \end{pmatrix}, \\ \mu_1{}^i = \begin{pmatrix} |b_1(e_2{}^i - e_1{}^i) + b_1\lambda_2{}^r y_1{}^i + b_1\lambda_2{}^i y_1{}^r \\ -b_1\lambda_1{}^r x_1{}^i - b_1\lambda_1{}^i x_1{}^r - a_1\lambda_1{}^r y_1{}^i \\ +a_1\lambda_1{}^r x_1{}^i - a_1\lambda_1{}^i y_1{}^r + a_1\lambda_1{}^i x_1{}^r| \end{pmatrix}, \\ \mu_2{}^r = \begin{pmatrix} |(b_2-b_1)e_1{}^r + b_2e_2{}^r + (b_2-b_1)\lambda_1{}^r x_1{}^r \\ -(b_2-b_1)\lambda_1{}^i x_1{}^i - e_1{}^r e_3{}^r - e_1{}^r\lambda_3{}^r z_1{}^r - \lambda_1{}^r x_1{}^r e_3{}^r \\ -\lambda_1{}^r x_1{}^r\lambda_3{}^r z_1{}^r + \lambda_1{}^i x_1{}^i e_3{}^r + \lambda_1{}^i x_1{}^i\lambda_3{}^r z_1{}^r \\ +b_2\lambda_2{}^r y_1{}^r - b_2\lambda_2{}^i y_1{}^i - \lambda_2{}^r a_2 x_1{}^r + \lambda_2{}^r y_1{}^r \\ +\lambda_2{}^r x_1{}^r z_1{}^r + \lambda_2{}^i a_2 x_1{}^i - \lambda_2{}^i y_1{}^i - \lambda_2{}^i x_1{}^i z_1{}^r| \end{pmatrix}, \\ \mu_2{}^i = \begin{pmatrix} |(b_2-b_1)e_1{}^i + b_2e_2{}^i + (b_2-b_1)\lambda_1{}^r x_1{}^i \\ +(b_2-b_1)\lambda_1{}^i x_1{}^r - e_1{}^i e_3{}^r - e_1{}^i\lambda_3{}^r z_1{}^r - \lambda_1{}^r x_1{}^i e_3{}^r \\ -\lambda_1{}^r x_1{}^i\lambda_3{}^r z_1{}^r - \lambda_1{}^i x_1{}^r e_3{}^r - \lambda_1{}^i x_1{}^r\lambda_3{}^r z_1{}^r \\ +b_2\lambda_2{}^r y_1{}^i + b_2\lambda_2{}^i y_1{}^r - \lambda_2{}^r a_2 x_1{}^i + \lambda_2{}^r y_1{}^i \\ +\lambda_2{}^r x_1{}^i z_1{}^r - \lambda_2{}^i a_2 x_1{}^r + \lambda_2{}^i y_1{}^r + \lambda_2{}^i x_1{}^r z_1{}^r| \end{pmatrix}, \\ \mu_3{}^r = \begin{pmatrix} |-b_3e_3{}^r + e_1{}^r e_2{}^r + e_1{}^r\lambda_2{}^r y_1{}^r - e_1{}^r\lambda_2{}^i y_1{}^i \\ +\lambda_1{}^r x_1{}^r e_2{}^r + \lambda_1{}^r x_1{}^r\lambda_2{}^r y_1{}^r - \lambda_1{}^r x_1{}^r\lambda_2{}^i y_1{}^i \\ -\lambda_1{}^i x_1{}^i e_2{}^r - \lambda_1{}^i x_1{}^i\lambda_2{}^r y_1{}^r + \lambda_1{}^i x_1{}^i\lambda_2{}^i y_1{}^i \\ +e_1{}^i e_2{}^i + e_1{}^i\lambda_2{}^r y_1{}^i + e_1{}^i\lambda_2{}^i y_1{}^r + \lambda_1{}^r x_1{}^i e_2{}^i \\ +\lambda_1{}^r x_1{}^i\lambda_2{}^r y_1{}^i + \lambda_1{}^r x_1{}^i\lambda_2{}^i y_1{}^r + \lambda_1{}^i x_1{}^r e_2{}^i \\ +\lambda_1{}^i x_1{}^r\lambda_2{}^r y_1{}^i + \lambda_1{}^i x_1{}^r\lambda_2{}^i y_1{}^r - b_3\lambda_3{}^r z_1{}^r \\ -\lambda_3{}^r x_1{}^r y_1{}^r - \lambda_3{}^r x_1{}^i y_1{}^i + a_3\lambda_3{}^r z_1{}^r| \end{pmatrix} \end{cases} \tag{20}$$

where $|.|$ denotes the absolute value. Then, we choose a Lyapunov function candidate as follows:

$$V(t) = {}^1\!/_2 \left(\sum_{k=1}^{3}(e_k{}^r)^2 + \sum_{k=1}^{2}(e_k{}^i)^2\right) \tag{21}$$

$$\dot{V}(t) = e_1{}^r\dot{e}_1{}^r + e_1{}^i\dot{e}_1{}^i + e_2{}^r\dot{e}_2{}^r + e_2{}^i\dot{e}_2{}^i + e_3{}^r\dot{e}_3{}^r \tag{22}$$

By substituting (13) into (22) and using (20), then one can obtain:

$$\dot{V}(t) \le \mu_1{}^r e_1{}^r + \mu_1{}^i e_1{}^i + \mu_2{}^r e_2{}^r + \mu_2{}^i e_2{}^i + \mu_3{}^r e_3{}^r + e_1{}^r\phi_1(u_1{}^r) + e_1{}^i\phi_1(u_1{}^i) + e_2{}^r\phi_2(u_2{}^r) + e_2{}^i\phi_2(u_2{}^i) + e_3{}^r\phi_3(u_3{}^r) \le \mu_1{}^r|e_1{}^r| + \mu_1{}^i|e_1{}^i| + \mu_2{}^r|e_2{}^r| + \mu_2{}^i|e_2{}^i| + \mu_3{}^r|e_3{}^r| + e_1{}^r\phi_1(u_1{}^r) + e_1{}^i\phi_1(u_1{}^i) + e_2{}^r\phi_2(u_2{}^r) + e_2{}^i\phi_2(u_2{}^i) + e_3{}^r\phi_3(u_3{}^r) \tag{23}$$

According to (11) and (19), then we have the following results:

$$\begin{cases} If \begin{pmatrix} e_k{}^r < 0 \text{ then } u_k{}^r > b_+, \text{so it conclude } (u_k{}^r - b_+)\phi_k(u_k{}^r) \ge (u_k{}^r - b_+)^2, \\ (u_k{}^r - b_+)\phi_k(u_k{}^r) = -\beta\mu_k{}^r sgn(e_k{}^r)\phi_k(u_k{}^r) \ge \beta^2(\mu_k{}^r)^2(sgn(e_k{}^r))^2 \end{pmatrix}, \\ If \begin{pmatrix} e_k{}^i < 0 \text{ then } u_k{}^i > b_+, \text{so it conclude } (u_k{}^i - b_+)\phi_k(u_k{}^i) \ge (u_k{}^i - b_+)^2, \\ (u_k{}^i - b_+)\phi_k(u_k{}^i) = -\beta\mu_k{}^i sgn(e_k{}^i)\phi_k(u_k{}^i) \ge \beta^2(\mu_k{}^i)^2\left(sgn(e_k{}^i)\right)^2 \end{pmatrix}, \\ If \begin{pmatrix} e_k{}^r > 0 \text{ then } u_k{}^r < -b_-, \text{ so it conclude } (u_k{}^r + b_-)\phi_k(u_k{}^r) \ge (u_k{}^r + b_-)^2, \\ (u_k{}^r + b_-)\phi_k(u_k{}^r) = -\beta\mu_k{}^r sgn(e_k{}^r)\phi_k(u_k{}^r) \ge \beta^2(\mu_k{}^r)^2(sgn(e_k{}^r))^2 \end{pmatrix}, \\ If \begin{pmatrix} e_k{}^i > 0 \text{ then } u_k{}^i < -b_-, \text{ so it conclude } (u_k{}^i + b_-)\phi_k(u_k{}^i) \ge (u_k{}^i + b_-)^2, \\ (u_k{}^i + b_-)\phi_k(u_k{}^i) = -\beta\mu_k{}^i sgn(e_k{}^i)\phi_k(u_k{}^i) \ge \beta^2(\mu_k{}^i)^2\left(sgn(e_k{}^i)\right)^2 \end{pmatrix} \end{cases} \tag{24}$$

Since $(e_k{}^r)^2 \ge 0, (e_k{}^i)^2 \ge 0$ and $e_k{}^r sgn(e_k{}^r) = |e_k{}^r|$, $e_k{}^i sgn(e_k{}^i) = |e_k{}^i|$ then from (24) we have:

$$\begin{cases} \begin{cases} -\beta\mu_k{}^r(e_k{}^r)^2 sgn(e_k{}^r)\phi_k(u_k{}^r) \\ = -\beta\mu_k{}^r(e_k{}^r)|e_k{}^r|\phi_k(u_k{}^r) \ge \beta^2(\mu_k{}^r)^2(e_k{}^r)^2\left(sgn(e_k{}^r)\right)^2 \end{cases} \\ \begin{cases} -\beta\mu_k{}^i(e_k{}^i)^2 sgn(e_k{}^i)\phi_k(u_k{}^i) \\ = -\beta\mu_k{}^i(e_k{}^i)|e_k{}^i|\phi_k(u_k{}^i) \ge \beta^2(\mu_k{}^i)^2(e_k{}^i)^2\left(sgn(e_k{}^i)\right)^2 \end{cases} \end{cases} \tag{25}$$

then one can conclude that

$$\begin{cases} e_k{}^r\phi_k(u_k{}^r) \le -\beta\mu_k{}^r|e_k{}^r| \\ e_k{}^i\phi_k(u_k{}^i) \le -\beta\mu_k{}^i|e_k{}^i| \end{cases} \tag{26}$$

Therefore, by substituting (26) into (23), one can obtain

$$\dot{V}(t) \le \sum_{k=1}^{3}\left(\mu_k{}^r|e_k{}^r| + e_k{}^r\phi_k(u_k{}^r)\right) + \sum_{k=1}^{2}\left(\mu_k{}^i|e_k{}^i| + e_k{}^i\phi_k(u_k{}^i)\right) \le \sum_{k=1}^{3}(\mu_k{}^r - \beta\mu_k{}^r)|e_k{}^r| + \sum_{k=1}^{2}(\mu_k{}^i - \beta\mu_k{}^i)|e_k{}^i| \tag{27}$$

If $\beta > 1$ then $\dot{V}(t) < 0$; which indicates that the stability of the system is guaranteed.

5. SIMULATION RESULTS

In this section, in order to verify the effectiveness and feasibility of the proposed synchronization scheme, the HCPS between two non-identical complex chaotic Lorenz system as drive system and complex chaotic Chen system as response system is accomplished, in which control input is subjected to dead-zone nonlinearity. The control inputs become active at $t = 5\ s$. For the case of HCPS, fourth-order Runge-Kutta method with initial conditions $\left(x_1{}^r(0) + jx_1{}^i(0), y_1{}^r(0) + jy_1{}^i(0), z_1{}^r(0)\right)^T = (1 + j2, 3 + j0.5, 4)^T$, $\left(x_2{}^r(0) + jx_2{}^i(0), y_2{}^r(0) + jy_2{}^i(0), z_2{}^r(0)\right)^T = (4.7 + j6, 0.2 + j7.5, 1)^T$ and time step size of 0.001 are used.

(21)

The scaling matrix is chosen as:

$\Lambda = diag\{1 + j0.5, 1 - j,\ 1.5\}$;

The control inputs containing dead-zone nonlinearity are defined as:

$$\begin{cases} \phi_k(u_k{}^r) = \begin{cases} (u_k{}^r - 1);\ u_k{}^r > 1, \\ 0; \quad -1 \le u_k{}^r \le 1, \\ (u_k{}^r + 1);\ u_k{}^r < -1 \end{cases} \quad, k = 1,2,3 \\ \phi_k(u_k{}^i) = \begin{cases} (u_k{}^i - 1);\ u_k{}^i > 1, \\ 0; \quad -1 \le u_k{}^i \le 1, \\ (u_k{}^i + 1);\ u_k{}^i < -1 \end{cases} \quad, k = 1,2 \end{cases} \tag{28}$$

Figure 4 displays the synchronized states of the complex chaotic Lorenz and Chen systems, where the control inputs are subjected to dead-zone nonlinearity. It is clear that the synchronization errors converge to zero quickly, which implies that the chaos synchronization between the complex chaotic Lorenz and Chen systems is realized, as shown in Figure 5. In this case, control parameters are selected as: $k_i = 10, i = 1,2, \ldots, 5$.

Figures 6 and 7 illustrate the synchronization errors between the complex chaotic Lorenz and Chen systems when the control parameters are selected as: $k_i = 20$ and $k_i = 30$ for $i = 1,2, \ldots, 5$, respectively.

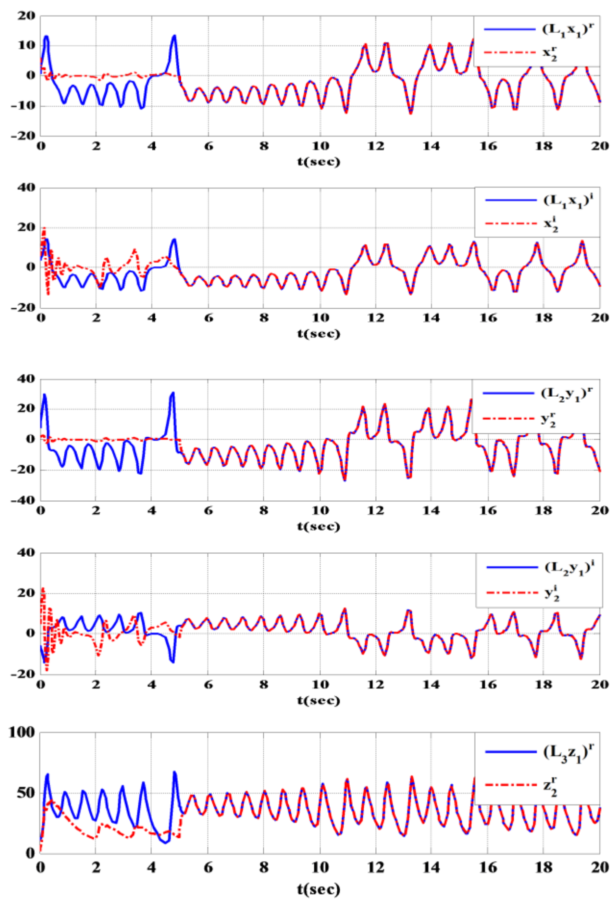

Fig. 4. State trajectories of complex chaotic Lorenz and Chen systems when $k_i = 10, i = 1,2, \ldots, 5$

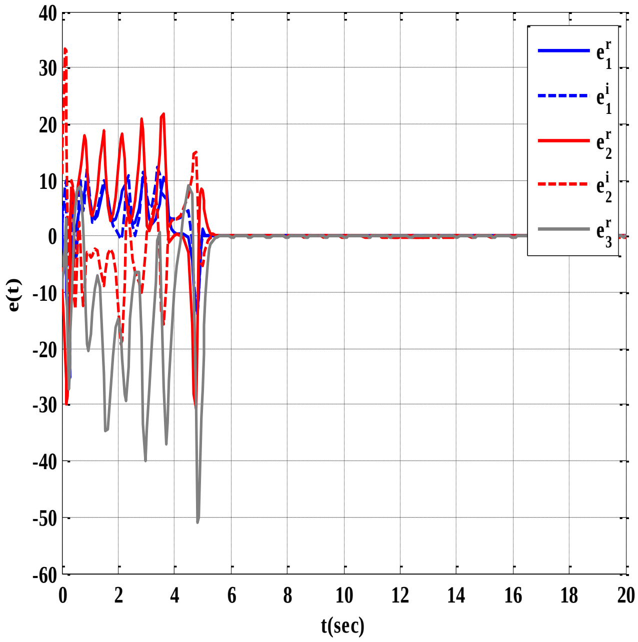

Fig. 5. Synchronization errors between the Lorenz and Chen systems when $k_i = 10, i = 1,2, \ldots ,5$

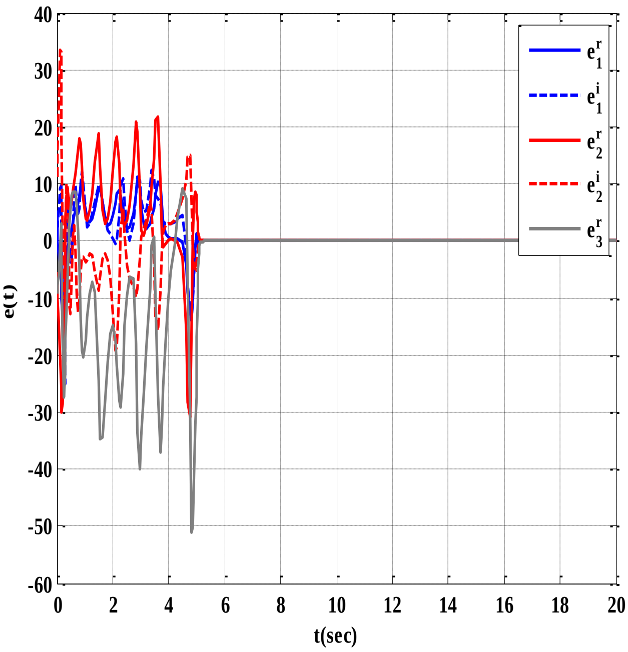

Fig. 7. Synchronization errors between the Lorenz and Chen systems when $k_i = 30, i = 1,2, \ldots ,5$

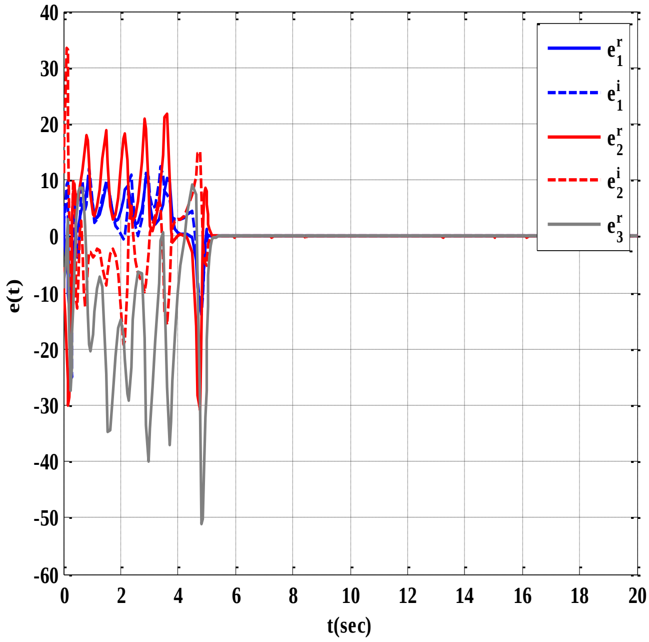

Fig. 6. Synchronization errors between the Lorenz and Chen systems when $k_i = 20, i = 1,2, \ldots ,5$

From the simulation results, it can be seen that the system error states asymptotically vanish, even in the presence of dead-zone nonlinearity in the control inputs. Also, it is obvious from Figs. 5 to 7 that by using the larger control parameter k_i, the error states converge toward zero faster and the synchronization errors decrease.

6. CONCLUSIONS

In this paper, an active nonlinear controller subject to input nonlinearity has been addressed. Based on the Lyapunov stability theorem, sufficient conditions to guarantee stable synchronization are given and the components of the error system tend to zero as time becomes large. Numerical simulations reveal that the proposed controller works well for chaos synchronization between two different complex chaotic systems even when there are nonlinearities in the control inputs.

REFERENCES

Bai, E.W., Lonngren, K.E., and Ucar, A. (2005). Secure communication via multiple parameter modulation in a delayed chaotic system. *Chaos, Solit. Fract.*, (23), 1071-1076.

Breve, F.A., Zhao, L., Quiles, M.G., and Macau, E.E.N. (2009). Chaotic phase synchronization and desynchronization in an oscillator network for object selection. *Neural Netw.*, (22), 728-737.

Das, S., Srivastava, M., and Leung, A.Y.T. (2013). Hybrid phase synchronization between identical and non-identical three-dimensional chaotic systems using the active control method. *Nonlinear Dyn.*, (73), 2261-2272.

Djari, A., Bouden, T., and Boulkroune, A. (2014). Design of fractional-order sliding mode controller (FSMC) for a class of fractional-order non-linear commensurate systems using a particle swarm optimization (PSO) Algorithm. *Journal of Control Engineering and Applied Informatics*, (16), 46-55.

Faieghi, M.R., and Delavari, H. (2012a). Chaos in fractional-order Genesio-Tesi system and its synchronization. *Commun. Nonlinear Sci. Numer. Simul*., (17), 731-741.

Faieghi, M.R., Delavari, H., and Baleanu, D. (2012b). Control of an uncertain fractional-order Liu System via fuzzy fractional-order sliding mode control. *J. Vib. Control*, (18), 1366-1374.

Feki, M. (2003). An adaptive chaos synchronization scheme applied to secure communication. *Chaos, Solit. Fract*., (18), 141-148.

Florin, A. and Silvia, A., (2011). Synchronizing robot motions in cooperative tasks. *Journal of Control Engineering and Applied Informatics*, (13), 43-48.

Hu, M., Yang, Y., Xu, Z., and Guo, L. (2008). Hybrid projective synchronization in a chaotic complex nonlinear system. *Math. Comput. Simulation*, (79), 449-457.

Huang, L., Feng, R., and Wang, M. (2004). Synchronization of chaotic systems via nonlinear control. *Phys. Lett. A* (320), 271-275.

Kebriaei, H., and Yazdanpanah, M.J. (2010). Robust adaptive synchronization of different uncertain chaotic systems subject to input nonlinearity. *Commun. Nonlinear Sci. Numer. Simulat*., (15), 430-441.

Li, H. et al., (2011). Adaptive Synchronization of Noise Perturbed Complex Delayed Network Systems. *Journal of Control Engineering and Applied Informatics*, (13), 3-8.

Li, J., Li, W., and Li, Q. (2012). Sliding mode control for uncertain chaotic systems with input nonlinearity. *Commun. Nonlinear Sci. Numer. Simulat*., (17), 341-348.

Luo, C., and Wang, X.Y. (2013a). Hybrid modified function projective synchronization of two different dimensional complex nonlinear systems with parameters identification. *J. Franklin Inst*., (350), 2646-2663.

Luo, C., and Wang, X.Y. (2013b). Hybrid robust modified function projective lag synchronization in two different dimensional chaotic systems. *Nonlinear Dyn*., (73), 245-257.

Mahmoud, G.M., Al-Kashif, M.A., and Aly, S.A. (2007a). Basic properties and chaotic synchronization of complex Lorenz system. *Int. J. Mod. Phys. C*, (18), 253-265.

Mahmoud, G.M., Bountis, T., and Mahmoud, E.E. (2007b). Active control and global synchronization for complex Chen and Lu systems. *Int. J. Bifurc. Chaos*, (17), 4295-4308.

Mahmoud, G.M., Ahmed, M.E., and Mahmoud, E.E. (2008). Analysis of hyperchaotic complex Lorenz systems. *Int. J. Mod. Phys. C*, (19), 1477-1499.

Márton, L. (2009). Adaptive friction compensation in the presence of backlash. *Journal of Control Engineering and Applied Informatics*, (11), 3-9.

Mohadeszadeh, M., and Delavari, H. (2015). Synchronization of fractional-order hyper-chaotic systems based on a new adaptive sliding mode control. *Int. J. Dynam. Control*, doi: 10.1007/s40435-015-0177-y.

Mohadeszadeh, M., and Delavari, H. (2015). Synchronization of uncertain fractional-order hyper-chaotic systems via a novel adaptive interval type-2 fuzzy active sliding mode controller. *Int. J. Dynam. Control*, doi: 10.1007/s40435-015-0207-9.

Murali, K., and Lakshmanan, M. (2003). Secure communication using a compound signal using sampled-data feedback. *Appl. Math. Mech.*, (11), 1309-1315.

Odibat, Z.M. (2010). Adaptive feedback control and synchronization of non-identical chaotic fractional order systems. *Nonlinear Dyn*., (60), 479-487.

Park, J.H., and Kwon, O.M. (2005). A novel criterion for delayed feedback control of time-delay chaotic systems. *Chaos, Solit. Fract.*, (23), 495-501.

Pecora, L.M., and Carroll, T.L. (1990). Synchronization in chaotic systems. *Phys. Rev. Lett.*, (64), 821-824.

Peng, G., Jiang, Y., and Chen, F. (2008). Projective synchronization of Chua's chaotic systems with dead-zone in the control input. *Math. Comput. Simulation*, 77, 374-382.

Roopaei, M., Zolghadri-Jahromi, M., John, R., and Lin, T.C. (2010). Unknown nonlinear chaotic gyros synchronization using adaptive fuzzy sliding mode control with unknown dead-zone input. *Commun. Nonlinear Sci. Numer. Simulat*., (15), 2536-2545.

Setoudeh, F., and Dousti, M. (2014). Chaos behavior of voltage control oscillator based on colpitts oscillator. *Journal of Control Engineering and Applied Informatics*, (16), 91-98.

Shutang, L., and Fangfang, Z. (2014). Complex function projective synchronization of complex chaotic system and its applications in secure communication. *Nonlinear Dyn*., (76), 1087-1097.

Srivastava, M., Ansari, S.P., Agrawal, S.K., Das, S., and Leung, A.Y.T. (2014). Anti-synchronization between identical and non-identical fractional-order chaotic systems using active control method. *Nonlinear Dyn*., (11), 905-914.

Sun, J.W., Cui, G.Z., Wang, Y.F., and Shen, Y. (2014). Combination complex synchronization of three chaotic complex systems. *Nonlinear Dyn*. doi: 10.1007/s11071-014-1714-5.

Sun, Z.Y., Si, G.Q., Min, F., and Zhang, Y. (2012). Adaptive modified function projective synchronization and parameter identification of uncertain hyperchaotic (chaotic) systems with identical or non-identical structures. *Nonlinear Dyn*., (68), 471-486.

Wei, Q., Wang, X.Y., Hu, X.P., and Feng, M.K. (2013). Adaptive hybrid complex projective synchronization of chaotic complex system. *J. Vib. Control*, (36), 1093-1097.

Wu, X., and Lü, J. (2003). Parameter identification and back-stepping control of uncertain Lü system. *Chaos, Solit. Fract*., (18), 721-729.

Wu, X., and Li, J. (2010). Chaos control and synchronization of a three species food chain model via Holling functional response. *Int. J. Comput. Math*., (87), 199-214.

Wu, X.J., Wang, H., and Lu, H. (2012). Modified generalized projective synchronization of a new fractional-order hyperchaotic system and its application to secure communication. *Nonlinear Anal. Real World Appl*., (13), 1441-1450.